Cancer Cell
Article

Acquisition of Granule Neuron Precursor Identity Is a Critical Determinant of Progenitor Cell Competence to Form Shh-Induced Medulloblastoma

Ulrich Schüller,[1,5,14] Vivi M. Heine,[1,6,7,14] Junhao Mao,[10] Alvin T. Kho,[11] Allison K. Dillon,[1] Young-Goo Han,[7] Emmanuelle Huillard,[1,6,7] Tao Sun,[1] Azra H. Ligon,[3,13] Ying Qian,[4] Qiufu Ma,[4] Arturo Alvarez-Buylla,[7,8] Andrew P. McMahon,[10] David H. Rowitch,[1,6,7,8,9,*] and Keith L. Ligon[1,2,3,12,13,*]
[1]Department of Pediatric Oncology
[2]Department of Medical Oncology
[3]Center for Molecular Oncologic Pathology
[4]Department of Cell Biology
Dana-Farber Cancer Institute, Harvard Medical School, Boston, MA 02115, USA
[5]Center for Neuropathology and Prion Research, Ludwig-Maximilians-Universität, Feodor-Lynen-Strasse 23, 81377 Munich, Germany
[6]Howard Hughes Medical Institute
[7]Institute for Regeneration Medicine
[8]Department of Neurological Surgery
[9]Department of Pediatrics
University of California, San Francisco, San Francisco, CA 94143, USA
[10]Department of Molecular and Cellular Biology, Harvard University, Cambridge, MA 02138, USA
[11]Informatics Program
[12]Department of Pathology
Children's Hospital Boston, Boston, MA 02115, USA
[13]Department of Pathology, Brigham and Women's Hospital, Boston, MA 02115, USA
[14]These authors contributed equally to this work
*Correspondence: rowitchd@peds.ucsf.edu (D.H.R.), keith_ligon@dfci.harvard.edu (K.L.L.)
DOI 10.1016/j.ccr.2008.07.005

SUMMARY

Whether the brain tumor medulloblastoma originates from stem cells or restricted progenitor cells is unclear. To investigate this, we activated oncogenic Hedgehog (Hh) signaling in multipotent and lineage-restricted central nervous system (CNS) progenitors. We observed that normal unipotent cerebellar granule neuron precursors (CGNPs) derive from *hGFAP*$^+$ and *Olig2*$^+$ rhombic lip progenitors. Hh activation in a spectrum of early- and late-stage CNS progenitors generated similar medulloblastomas, but not other brain cancers, indicating that acquisition of CGNP identity is essential for tumorigenesis. We show in human and mouse medulloblastoma that cells expressing the glia-associated markers Gfap and Olig2 are neoplastic and retain features of embryonic-type granule lineage progenitors. Thus, oncogenic Hh signaling promotes medulloblastoma from lineage-restricted granule cell progenitors.

INTRODUCTION

It has been proposed that cancer can be viewed as aberrant organogenesis initiated by a multipotent or restricted progenitor cell that acquires infinite capacity for self-renewal through accumulated mutations (Reya et al., 2001). Principles of normal hematopoietic stem cell development (Barabe et al., 2007; Cobaleda et al., 2007) have provided insight into the mechanisms of

SIGNIFICANCE

Cancer stem cells have been proposed as therapeutic targets in human brain cancer. Although such populations have been reported in medulloblastoma, tumor progenitor origins remain unclear. Here we show that medulloblastoma is generated from cells related to several stages of cerebellar granule neuron precursor (CGNP) development and that some tumor cells, demonstrable in murine models and human medulloblastoma, retain primitive features analogous to precursors of the embryonic brain. These data highlight the importance of a developmental perspective in understanding cells involved in central nervous system tumor progression and the histopathological composition of brain cancers. They suggest that a potential therapeutic target is the process regulating acquisition of CGNP phenotype.

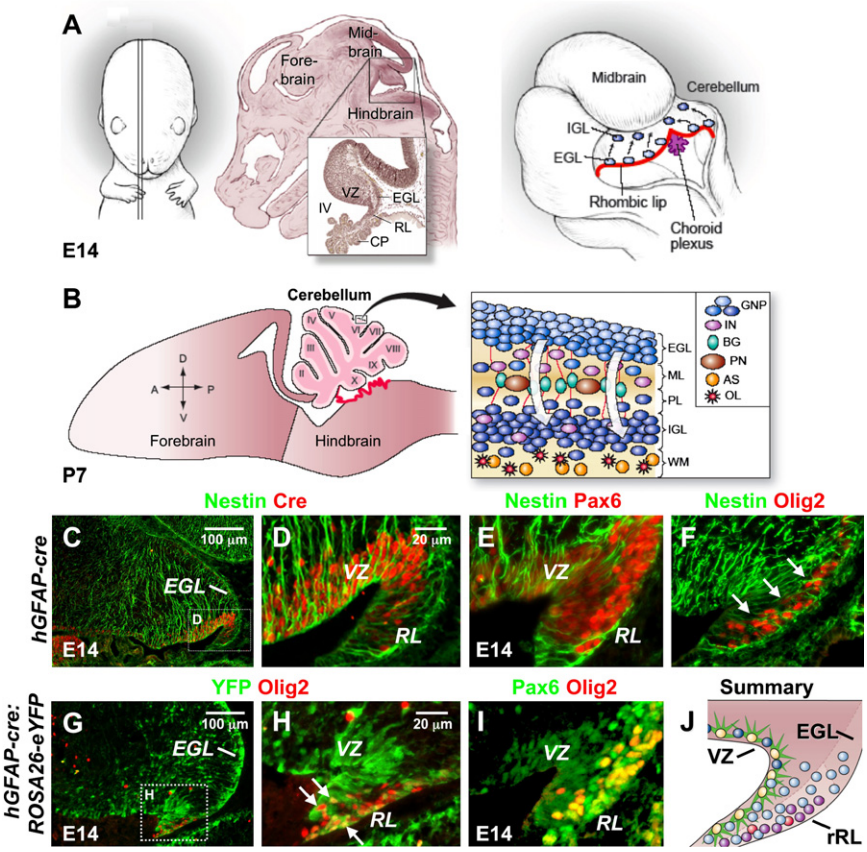

Figure 1. Identification of an Olig2$^+$ Progenitor Population in the Rostral RL

(A) The cerebellar anlage at E14. The ventricular zone (VZ) and rhombic lip (RL) serve as mitotic niches at this age. The external granule layer (EGL) is formed by proliferating cerebellar granule neuron precursors (CGNPs) that have left the RL. CP, choroid plexus; IGL, internal granule layer.

(B) At postnatal day 7 (P7), the developing cerebellum (CB) is divided into ten lobes with defined cortical layers. ML, molecular layer; PL, Purkinje cell layer; WM, white matter; GNP, granule neuron precursor; IN, interneuron; BG, Bergmann glia; PN, Purkinje neuron; AS, astrocyte; OL, oligodendrocyte.

(C–E) Sagittal sections at embryonic day 14 (E14) in *hGFAP-cre* mice showing colocalization of nestin, Cre, and Pax6 proteins in progenitor cells of the VZ and rostral rhombic lip (rRL).

(F) Olig2 expression is largely restricted to the dorsal rRL.

(G and H) Fate-mapping experiments (*hGFAP-cre* × *ROSA26-eYFP$^{flox/flox}$* mice) reveal yellow fluorescent protein (YFP) in the EGL and a subset of RL cells that express Olig2 (arrows).

(I) Olig2$^+$ RL precursors colabel with the CGNP marker Pax6; some single Pax6$^+$ precursors in the VZ were observed (arrows).

(J) Summary of cells in the rRL region at E14 showing relative positions of radial glia (yellow and green), Pax6$^+$ (light blue and dark blue), Olig2$^+$ (red), and Pax6$^+$Olig2$^+$ (purple) cells.

self-renewal and multilineage differentiation in hematopoietic malignancies (Faber and Armstrong, 2007; Warner et al., 2004). However, for most organ systems, parallels between normal stem cell development and solid tumor formation remain poorly understood.

The central nervous system (CNS), with its highly diversified classes of neuronal and glial progenitor cells, provides a suitable model to study such mechanisms. Several studies have documented the existence of cancer stem cells for glioma and the cerebellar tumor medulloblastoma (MB) with properties reminiscent of normal neural precursors (Singh et al., 2004; Galli et al., 2004; Hemmati et al., 2003). Expression profiling has indicated correlations between specific stages of cerebellar development and MB (Lee et al., 2003; Kho et al., 2004). The Sonic hedgehog (Shh) pathway has critical functions in cerebellar development, and mutations of this pathway are etiologic in MB (Pietsch et al., 1997).

The cerebellum (CB) develops from several progenitor regions, the rostral rhombic lip (rRL) and cells of the ventricular zone (VZ) surrounding the IVth ventricle (Altmann and Bayer, 1997; Morales and Hatten, 2006; Kawauchi et al., 2006; Casper and McCarthy, 2006; Malatesta et al., 2003) (Figure 1A). The VZ of the cerebellar anlage generates Purkinje neurons (PNs), interneurons (INs), and glial cells. Progenitors within the rRL express the radial glial markers RC2 and nestin and give rise to all granule lineage cells (GCs) of the external granule layer (EGL) and internal granule layer (IGL). We recently reported that cells that express Cre recombinase under control of human regulatory sequences for glial fibrillary acidic protein (*hGFAP*) are most probably radial glia and generate most cerebellar cell types, including cerebellar granule neuron precursors (CGNPs) (Spassky et al., 2008). Subsequently, CGNPs migrate rostrally along the surface of the cerebellar anlage to form the EGL (Lee et al., 2005; Machold and Fishell, 2005; Wang et al., 2005) (Figure 1A).

PNs (Figure 1B) produce Shh, which binds the transmembrane protein repressor Patched (Ptc), relieving inhibition of Smoothened (Smo) activity, which is essential for CGNP proliferation in the EGL (Wechsler-Reya and Scott, 1999; Dahmane and Altaba, 1999; Lewis et al., 2004). CGNPs of the EGL gradually show reduced proliferation levels, migrate internally, and differentiate into glutamatergic neurons in the IGL (Figure 1B), a process that is largely completed by postnatal day 15 (P15) in mice (Borghesani et al., 2002), and by about one year of age in the human CB (Abraham et al., 2001). Transcriptional control of CGNP development involves functions of the bHLH protein Math1 (Ben Arie et al., 1997; Machold and Fishell, 2005; Wang et al., 2005) and the homeodomain protein Pax6 (Engelkamp et al., 1999; Yamasaki et al., 2001).

Inherited activating mutations of the Shh/Smo pathway in humans are etiologic in MB, but not in glioma (Hahn et al., 1999; Johnson et al., 1996). This cancer spectrum is faithfully modeled in the CNS of mice heterozygous for a mutation of the Hedgehog (Hh) pathway suppressor *Ptc* (Johnson et al., 1996) or expressing an activated allele of *Smoothened* (*SmoM2*) (Mao et al., 2006), supporting the proposal that CGNPs are particularly susceptible to transformation by oncogenic Hh signaling (Shih and

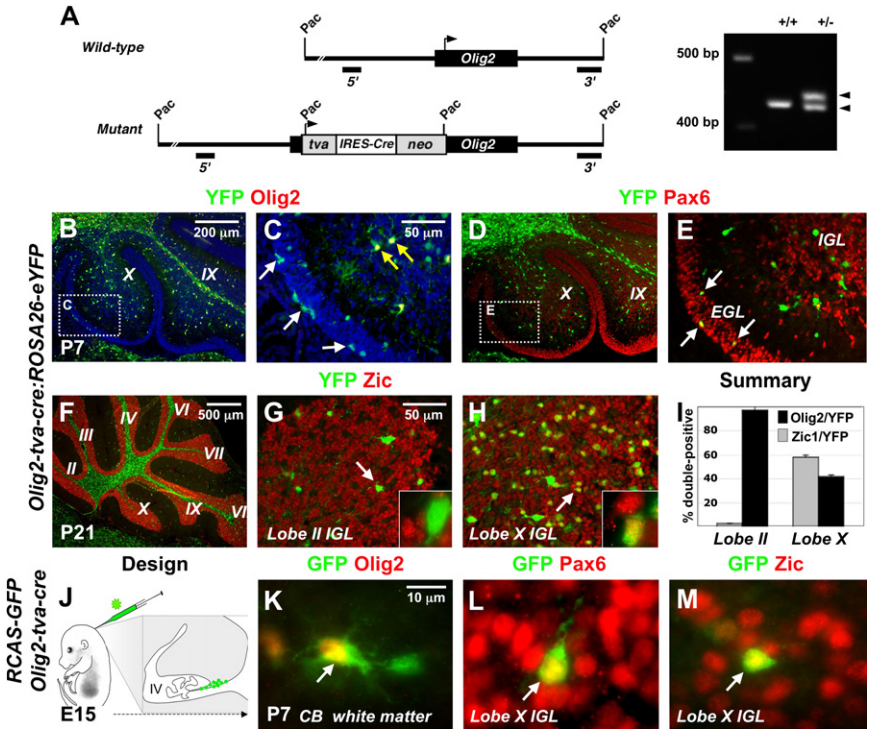

Figure 2. A Subset of Cerebellar Granule Neurons Derive from Olig2$^+$ Progenitors

(A) The *Olig2-tva-cre* allele and genotyping of the respective mutant mice using PCR to generate wild-type 429 bp and mutant (cre) 446 bp products.

(B–I) Fate mapping of Olig2-expressing cells with the *ROSA26-eYFP$^{flox/flox}$* reporter. Colocalization of YFP and Olig2 proteins in sagittal sections of P7 cerebella reveals that YFP is expressed in oligodendrocytes within the cerebellar WM (yellow arrows in C) as well as in occasional cells within the EGL (white arrows). YFP/Pax6 labeling confirms the granule lineage character of YFP-expressing EGL cells (D, arrows in E). The IGL of P21 cerebella demonstrates lobe-specific differences in Olig2 fate mapping.

(G) The IGL of lobe II contains YFP$^+$ cells that predominantly coexpress Olig2 (arrow and inset) but not the granule lineage cell (GC) marker Zic.

(H) In contrast, the IGL of lobe X contains numerous YFP/Zic double-positive cells (arrow and inset).

(I) Mean percentage (±SEM) of Olig2/YFP and Zic1/YFP double-positive cells in the IGL of lobe II and X.

(J–M) In utero fate mapping of Olig2-expressing cells by RCAS-GFP virus injection into the rRL of E15.5 *Olig2-tva-cre* mice. Analysis of the CB at P7 reveals GFP to be expressed in Olig2$^+$ (K) WM cells, as well as in Pax6$^+$ (L) and Zic$^+$ (M) cells of the IGL in lobe X.

Holland, 2004). Nevertheless, the cellular origins of MB from unipotent precursors in the EGL remain controversial. The identification of multipotent MB stem cells (Hemmati et al., 2003; Singh et al., 2004) capable of multilineage differentiation, in particular, has challenged the hypothesis of a unipotent cell of origin. To investigate these issues, we defined distinct progenitor populations for CGNPs within the rRL as well as in the EGL and systematically assessed their tumorigenic potential with respect to Hh signaling.

RESULTS

Olig2 Expression Identifies RL Progenitors for a Subset of Granule Cell Neurons

In order to determine possible parallels between progenitors during cerebellar development and tumorigenesis, we first characterized relevant embryonic hindbrain VZ and rhombic lip (RL) populations. Nuclei of cells that express Cre proteins in *hGFAP-cre* mice are observed along the VZ and the ventral aspect of the rRL of the midline cerebellar anlage at E14.5 (Figures 1C–1E). Cre proteins in these mice mark nestin$^+$ cells that have been proposed to be radial glia of the rRL that give rise to CGNPs (Spassky et al., 2008), which show robust Pax6 expression. We next investigated expression of the bHLH protein Olig2, which marks multilineage progenitor populations of the forebrain and the spinal cord (Petryniak et al., 2007; Lu et al., 2002; Zhou and Anderson, 2002). Olig2 expression identified a distinct cell population predominantly restricted to the rRL and extending to the boundary of the EGL (Figure 1F). The cerebellar VZ contained rare Olig2$^+$ cells, and expression of Olig2 was rapidly downregulated within the EGL.

To establish a possible lineage relationship between *hGFAP-cre* and Olig2$^+$ cells, we fate mapped *hGFAP-cre*-expressing precursors with a conditional *ROSA26-eYPF$^{flox/flox}$* reporter (Srinivas et al., 2001). As shown (Figure 1G, white line), *hGFAP-cre*-expressing precursors give rise to the majority of CGNPs of the primitive EGL and some Olig2$^+$ cells of the rRL (Figure 1H). Most Olig2$^+$ cells in the rRL coexpressed the CGNP marker Pax6 (Figure 1I), while Olig2 expression was gradually lost and Pax6 was retained as CGNPs migrated into the EGL. Olig2$^+$Pax6$^+$ cells could be identified within the rRL and EGL until E18.5 but were never observed at P7 or later stages (data not shown; see also below).

To establish *Olig2*$^+$ progenitor contributions during CGNP development, we constructed a multifunctional mouse line by inserting *tva*, an avian-specific retroviral receptor, and an *IRES-cre* recombinase cassette into the endogenous *Olig2* locus by homologous recombination (Figure 2A). When *Olig2-tva-cre$^{+/-}$* mice were crossed to *ROSA26-eYFP$^{flox/flox}$* conditional reporter mice, we found that 98% of YFP$^+$ cells in the P7 cerebellar white matter (WM) expressed Olig2, consistent with oligodendroglial identity (Figures 2B and 2C, yellow arrows). At P21, most of these cells coexpressed myelin basic protein, and we observed small numbers of YFP$^+$ PNs and INs (see Figures S1E and S1F available online). At P7, we detected a small subpopulation of YFP$^+$ CGNPs within the EGL, confined mainly to posterior cerebellar lobes IX and X (Figures 2C–2E, white arrows). At P21, we observed fate mapping to GCs within the IGL (Figures 2F–2I). Interestingly, only 3% of YFP$^+$ cells expressed the GC marker Zic in the lobe II IGL, but 58% of YFP$^+$ cells were double positive in lobe X (Figures 2G and 2I), indicating that Olig2 contributions to GCs of the IGL are restricted mainly to the posterior lobes.

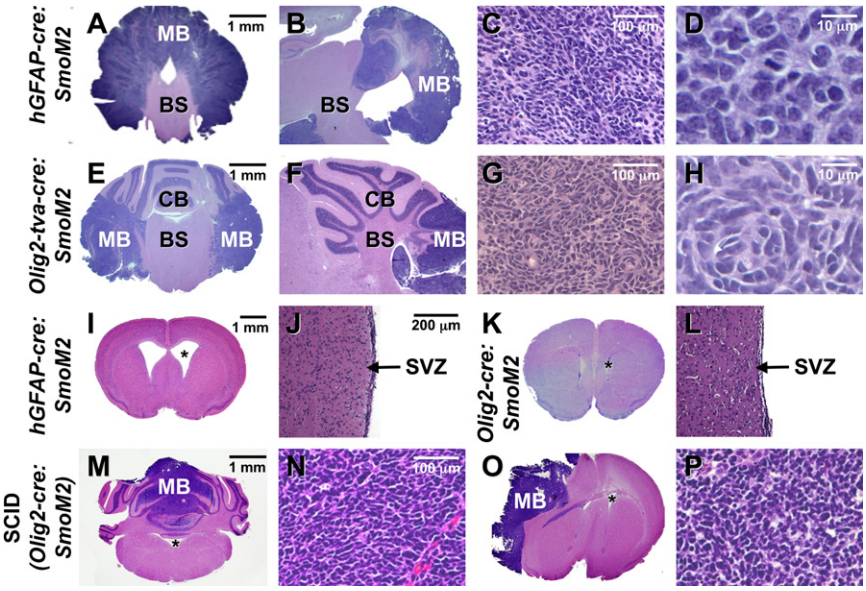

Figure 3. Development of Medulloblastoma but Not Glioma from *hGFAP*$^+$ and *Olig2*$^+$ Precursors

(A–H) Targeting *hGFAP*$^+$ and *Olig2*$^+$ precursor cells with SmoM2 results in medulloblastoma (MB). While neoplastic transformation of *hGFAP*$^+$ cells affects the entire cerebellar cortex (A–D), MBs from *Olig2*-expressing precursors are restricted to posterior cerebellar regions (E–H). Although *hGFAP-cre* and *Olig2-cre* are broadly expressed in all parts of the central nervous system, neoplastic lesions due to SmoM2 are restricted to the CB.

(I–L) Forebrain sections including the subventricular zone (SVZ) in adult animals appear normal.

(M–P) Transplantation of *Olig2-tva-cre:SmoM2* tumor cells into SCID mice gives rise tumors both in hindbrain (M and N) and forebrain (O and P) regions.

(A), (E), and (I)–(P) are frontal sections; (B)–(D), (F)–(H), (N), and (P) are sagittal sections stained with hematoxylin and eosin. (C) and (D) are high-power magnifications of (B), as are (G) and (H) from (F). Asterisks mark lateral ventricles in (I), (K), and (O) and the IVth ventricle in (M). BS, brainstem.

We found Olig2$^+$ cells in the rRL from E14.5 to E18.5 (Figure 1; data not shown). To test whether these cells in particular were a source of lobe IX/X CGNPs, we injected the rRL of E15.5 *Olig2-tva-cre*$^{+/-}$ animals with an avian retrovirus (RCAS-GFP) that can only transduce *tva*-expressing cells (Figure 2J). Fate-mapping results analyzed at P7 indicated that infected rRL *Olig2-tva*$^+$ cells generate Pax6$^+$ CGNPs of the EGL and Zic$^+$ GCs within the IGL (Figures 2K and 2M; Figure S1) of lobes IX and X. Taken together, these data indicate that *Olig2*$^+$ progenitors of the rRL make restricted contributions to the GC lineage, particularly in posterior lobes of the CB.

Smoothened Activation within CNS *hGFAP*$^+$ and *Olig2*$^+$ Progenitors Produces Only Medulloblastoma

To determine the significance of *hGFAP*- and *Olig2*-expressing progenitor populations for CNS tumorigenesis, we used *hGFAP-cre* and *Olig2-tva-cre* drivers, respectively, to conditionally express an activated *Smo* (*SmoM2*) allele fused with *YFP* sequences (Mao et al., 2006). All *hGFAP-cre:SmoM2* mice developed diffuse tumors with the characteristic "small round blue cell" histology of MB (Figures 3A–3D; Table 1). *Olig2-tva-cre:SmoM2* mice developed tumors with similar histology, except that they were focal, localized to the posterior-lateral lobes, and had significantly ($p < 0.01$) later mortality (Figures 3E–3H; Table 1), which was likely a result of their focal nature and the small numbers of CGNPs targeted by *Olig2-tva-cre*.

Although *hGFAP*$^+$ and *Olig2*$^+$ progenitor populations give rise, collectively, to CGNPs as well as INs, astrocytes (ASs), and oligodendrocytes (OLs), we only observed cerebellar tumors with histological features of MB. Additionally, activated Hh signaling in cerebellar PNs driven by *Shh-creERT2* did not result in MB (Table 1). These data demonstrate that *hGFAP*$^+$ and *Olig2*$^+$ multipotent progenitor populations can produce MB.

Hh signaling can have mitogenic effects in the spinal cord and forebrain (Mao et al., 2006; Rowitch et al., 1999; Fuccillo et al., 2006), and roles in forebrain glioma have been reported (Clement et al., 2007; Ehtesham et al., 2007). However, no evidence of gliomas or other primitive neuroectodermal tumors (PNETs) in the forebrain was observed despite forced expression of SmoM2 in the subventricular zone (SVZ), in NG2$^+$ progenitors, and in oligodendrocyte precursor cells (OPCs) of the forebrain (Figures 3I–3L; Table 1). Together, these data indicated a hindbrain- as well as a CGNP/lineage-restricted oncogenic response to Hh signaling and raised the question of whether this is determined by the particular environmental niche of the EGL. To assess this, we transplanted freshly dissociated cells from *Olig2-tva-cre:SmoM2* tumors into the forebrains and cerebella of SCID mice. Tumors formed equally well in both locations (Figures 3M–3P; Table 1), suggesting that tumor propagation is governed primarily by cell-intrinsic factors rather than environment.

Unipotent CGNPs Are Competent to Produce Medulloblastoma

In myeloid oncogenesis, multipotent cells rather than more restricted progenitor cells are thought to be the origin of leukemia stem cells (Faber and Armstrong, 2007). To test whether a restricted neuronal precursor can also give rise to MB, we activated SmoM2 in committed CGNPs. *Math1-cre* drives expression within CGNPs of the rRL and the entire EGL until P7–10, but not in PNs, ASs, or INs (Machold and Fishell, 2005; Wang et al., 2005). In contrast, expression of the transcription factor *Tlx3* (*Hox11L2*) is seen only in the EGL of lobes VI–IX, but not in other lobes or the rRL (Figure S2). Transgenic *Math1-cre* mice were generated using regulatory sequences 4 kb upstream of *Math1* (Matei et al., 2005), and *Tlx3-cre* mice were generated by gene targeting of *Tlx3* (Xu et al., 2008). Fate-mapping crosses involving a conditional *ROSA26-eYFP*$^{flox/flox}$ reporter confirmed that *Math1*$^+$ and *Tlx3*$^+$ precursors contributed solely to the GC lineage (Figures 4A–4H; data not shown).

Table 1. Summary of Phenotypes from Crosses of Various *cre* Drivers with *SmoM2*$^{flox/flox}$ Mice

Genotype	Transgene Type	n	MB Formation (%)	Average Survival (Days)	Tumor Location	Cerebellar Cell Types Targeted
Math1-cre	transgenic	63	100	41	diffuse	CGNPs (all lobes), deep cerebellar nuclei
Tlx3-cre	knockin	37	100	45	lobes VI–IX	lobe VI–IX CGNPs
Shh-creERT2	transgenic	10	0	NA	NA	Purkinje neurons
hGFAP-cre	transgenic	12	100	33	diffuse	radial glia, all CGNPs, interneurons, forebrain stem cells, astrocytes
Olig2-tva-cre	knockin	11	100	57	posterior-lateral	rostral rhombic lip progenitors, lobe X CGNPs, oligodendrocyte precursor cells, NG2 cells, interneurons
Gli1-creERT2	transgenic	10	40	102	focal	CGNPs, Bergmann glia
Olig2-tva-cre:SmoM2	transplant	5	NA	47	forebrain/hindbrain	NA
Math1-cre:SmoM2	transplant	3	NA	84	hindbrain	NA

The various *cre* drivers used, number of crosses performed, average onset of tumor-associated premorbid state, tumor location, and cells initially targeted by Cre recombinase are indicated. Tamoxifen induction was performed in *Shh-creERT2* and *Gli1-creERT2* mice at P10. Results of allotransplantation of *Olig2-tva-cre:SmoM2*- and *Math1-cre:SmoM2*-derived tumors are indicated. NA, not applicable; CGNP, cerebellar granule neuron precursor.

When crossed with *SmoM2*$^{flox/flox}$ mice, all *Math1-cre* animals developed MBs that could be transplanted into the cerebella of SCID mice (Figures 4I and 4J; Table 1; see also Yang et al. [2008] in this issue of *Cancer Cell*). *Tlx3-cre:SmoM2* animals developed tumors in a posterior distribution in accord with the *Tlx3* expression domain (Figures 4K and 4L). These data show that unipotent CGNPs are capable of tumor formation when targeted with oncogenic SmoM2. The Shh transcriptional target Gli1 is expressed in proliferating CGNPs (Wechsler-Reya and Scott, 1999), and we could induce MB formation in *Gli1-creERT2:SmoM2* mice until P14, but not at later postnatal stages (Table 1).

Medulloblastomas Exhibit a Common Phenotypic Endpoint despite Diverse Cellular Origins

To determine whether significant cellular (i.e., glial and neuronal diversity) and gene expression differences might exist in tumors derived from multipotent (e.g., *hGFAP-cre*) versus unipotent (e.g., *Math1-cre*) progenitor populations, we performed Affymetrix gene expression profiling analyses, previously demonstrated to aid in distinguishing MB from other histologically similar PNETs (Pomeroy et al., 2002). Comparison of expression profiles of the different murine tumors and *Ptc*$^{+/-}$ MB using principal component (PC) analysis confirmed that all tumors had a gene expression signature of MB and were highly related to each other (Figure 5A). Along the PC1 coordinate—the direction of greatest transcriptomic sample variance in cerebellar development—centroids of the MB tumor profiles were significantly different from matched normal samples ($p < 10^{-6}$). However, PC1 coordinate centroids were not significantly different for tumors derived from early (i.e., *hGFAP-cre* or *Olig2-cre*) versus late/unipotent (i.e., *Math1-cre* or *Tlx3-cre*) GC lineage progenitors (Figure S3). In fact, only a very small number of genes (~150 of 54,675 probes tested) were found to be uniquely and differentially expressed in each tumor subgroup. In line with this, extensive histological (Figures 3C and 3G; Figures 4J and 4L) and immunohistochemical analysis (Figure 5B) failed to reveal any clear differences in the cellular composition of the tumors. Furthermore, hierarchical cluster analysis based on the 150 genes differentially expressed among the tumors did not show strict clustering of tumors based on cell of origin (Figure S4). Together, these findings indicate that tumors derived from early (i.e., *hGFAP-cre* or *Olig2-cre*) or late/unipotent (i.e., *Math1-cre* or *Tlx3-cre*) GC lineage progenitors arrive at a common phenotypic endpoint.

Cells Expressing Gfap and Olig2 in Hh-Activated Medulloblastomas Are Neoplastic

All mouse tumors analyzed exhibited histological features in common with some human MBs, including expression of CGNP markers (Math1, Zic, and Pax6); Gfap, a marker usually found to be expressed in ASs; and Olig2, which is required for OL development (Lu et al., 2002; Figure 5B). Clinical symptoms of tumor burden in *Math1-cre:SmoM2* tumors developed at an average age of 41 days (Table 1); however, we found evidence of hyperplasia in the EGL at P0 and more clearly at P7 (Figures 6A and 6C). Strikingly, high expression of Olig2 was also found in these regions (Figures 6B and 6D). At P7, when the EGL is clearly discernable, excessive numbers of Olig2^{+} cells were observed in the EGL but not the RL of *Math1-cre:SmoM2* mice (Figure 6D). Indeed, although Olig2^{+} cells that coexpressed Pax6 (Figure 1I) or a Math1 proxy marker (Figure 6E) could be observed at antenatal stages until E18, such colabeled cells were not detectable at P7 (Figure 6F) or later stages. Thus, persistent Olig2 expression in the EGL of *Math1-cre:SmoM2* mice represents an early molecular marker of a preneoplastic state.

We found that only about 2% of mitotically active phospho-H3^{+} (p-H3) cells were Olig2^{+} in fully developed *Math1-cre:SmoM2* tumors (Figure 6G). Indeed, the vast majority of

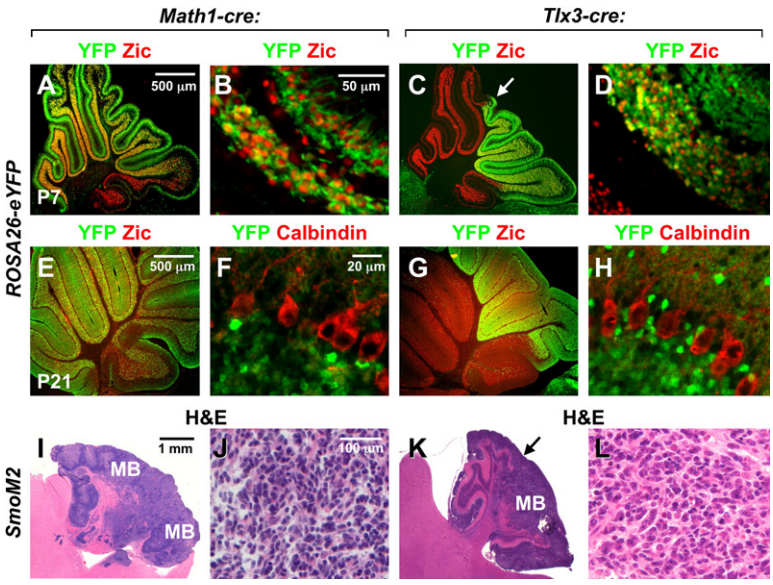

Figure 4. Late-Stage Unipotent CGNPs Are Competent to Produce Medulloblastoma

(A–H) Cre expression driven by *Math1* or *Tlx3* promoter sequences is normally restricted to GCs, as shown by crosses with *ROSA26-eYFP* conditional reporter mice.

(C, D, and G) GCs fate mapped by *Tlx3-cre* are restricted to lobes VI–IX.

(F and H) In contrast, calbindin-expressing Purkinje neurons do not derive from *Math1*$^+$ or *Tlx3*$^+$ precursors.

(I–L) Both *Math1*$^+$ and *Tlx3*$^+$ granule neurons give rise to MB after activation of SmoM2, and *Tlx3-cre*-driven tumors obeyed posterior restriction consistent with fate mapping (compare arrows in C and K).

proliferating cells were Cre$^+$ (Figure 6H), a proxy for *Math1* expression, indicating that most cells contributing to MB growth are CGNP-like. In human tumors, it is controversial whether cells expressing GFAP (or OLIG2) comprise the tumor or, alternatively, represent intermingled cells from the normal brain. This is a critical point given that glial differentiation within MB would provide further evidence for a multipotent stem cell-like progenitor. To establish the nature of cells comprising MB, we dissociated *Math1-cre:SmoM2* tumors and found that the SmoM2-YFP fusion protein, a marker of cells bearing the tumorigenic mutation, colocalized in cells expressing Pax6, NeuN, Gfap, or Olig2. Quantification revealed that YFP proteins colocalized with most if not all Pax6$^+$, Olig2$^+$, and Gfap$^+$ (100%, 90%, and 96%, respectively) cells in acutely dissociated tumors (Figures 6I–6L). In addition, we identified Olig2$^+$ and Gfap$^+$ cells that coexpressed the YFP reporter in vivo (Figures 6M and 6N). Thus, Olig2$^+$ and Gfap$^+$ cells are tumor cells rather than infiltrated/normal glial cells.

The Gfap$^+$ and Olig2$^+$ cells might represent simple astroglial and oligodendroglial tumor components. However, examination of Gfap$^+$ and Olig2$^+$ cells of the cerebellar anlage (Figure 1) suggested that such tumor cells could, alternatively, retain features of primitive CGNPs. In support of the latter possibility, we found that 81% of Olig2$^+$ cells expressed Pax6 and that 100% of Gfap$^+$ cells expressed Pax6 in acutely disassociated *Math1-cre:SmoM2* tumors in vitro (Figures 6O and 6P). These findings indicate that cells with an immature/progenitor phenotype are present in Hh-activated MB.

Human Medulloblastomas Contain Rare OLIG2$^+$ Cells with Progenitor Features

In order to determine the significance that our findings might have for human MB, we examined OLIG2$^+$ cell populations within a cohort of human MBs. Although our original findings in mice were all in the setting of Shh/Smo pathway activation, we found that OLIG2$^+$ cells were present in both classic (40%) and desmoplastic (Shh-related) (77%) subtypes of human MBs (Figures 7A–7D; Table S1) and comprised less than 5% of cells in all tumors. Fluorescence in situ hybridization (FISH) analysis showed that OLIG2$^+$ cells in human MB contained copy-number gain at the c-*MYC* locus, confirming these as tumor cells and arguing against the possibility that they might represent intermingled normal cells (Figures 7E and 7F). Further supporting that OLIG2$^+$ cells are tumor cells, we identified coexpression of OLIG2 and the terminal neuronal differentiation marker NEUN in rare cells within human tumors (Figure 7G), and we found rare OLIG2$^+$ cells that expressed the proliferation marker Ki-67 (Figure 7H). Together, these data suggest the possibility that some OLIG2$^+$ cells are tumor cells with immature features and may represent a type of MB progenitor cell.

To mechanistically assess the lineage differentiation potential of Olig2$^+$ cells in the context of MB, we acutely disassociated tumors from *Olig2-tva-cre:SmoM2* mice and infected these cultures with RCAS-GFP viruses to perform fate mapping of tumor stem/progenitor cells (Figure 7I). In our experimental paradigm, cells must be Olig2-tva$^+$ for infection with RCAS-GFP to occur. After 6 days in culture, we found that cells derived from Olig2$^+$ progenitors expressed Pax6, Zic, or NeuN (Figures 7K–7N). Significantly, of the 561 GFP$^+$ cells counted, only 68 (12%) expressed Olig2 on day 6 (Figures 7J and 7N), indicating differentiation along the GC lineage axis with downregulation of Olig2. Upon acute harvest and disassociation of tumors (day 0), we found that only 8% expressed Olig2. Of these, 66% coexpressed Pax6 and 12% expressed NeuN (Figures 7O–7Q). In contrast, on day 6 in the tva fate-mapping experiment, 52% of Olig2-derived progeny expressed NeuN. These data are consistent with the proposal that Olig2$^+$Pax6$^+$ cells lose Olig2 expression and progress to express the more mature markers such as Zic and NeuN during the 6 days in culture. We conclude that Olig2$^+$ cells in *Olig2-tva-cre:SmoM2* tumors have the potential to produce GC-like progeny, therefore supporting the possibility that they represent a subset of MB progenitor cells.

DISCUSSION

Here we show that unipotent CGNPs derive from multilineage embryonic CNS progenitors and that both populations are capable of generating MB when targeted with oncogenic SmoM2. Despite diverse origins, resulting tumors were similar, leading to the conclusion that acquisition of CGNP identity is a critical determinant of progenitor cell competence to form Hedgehog-induced

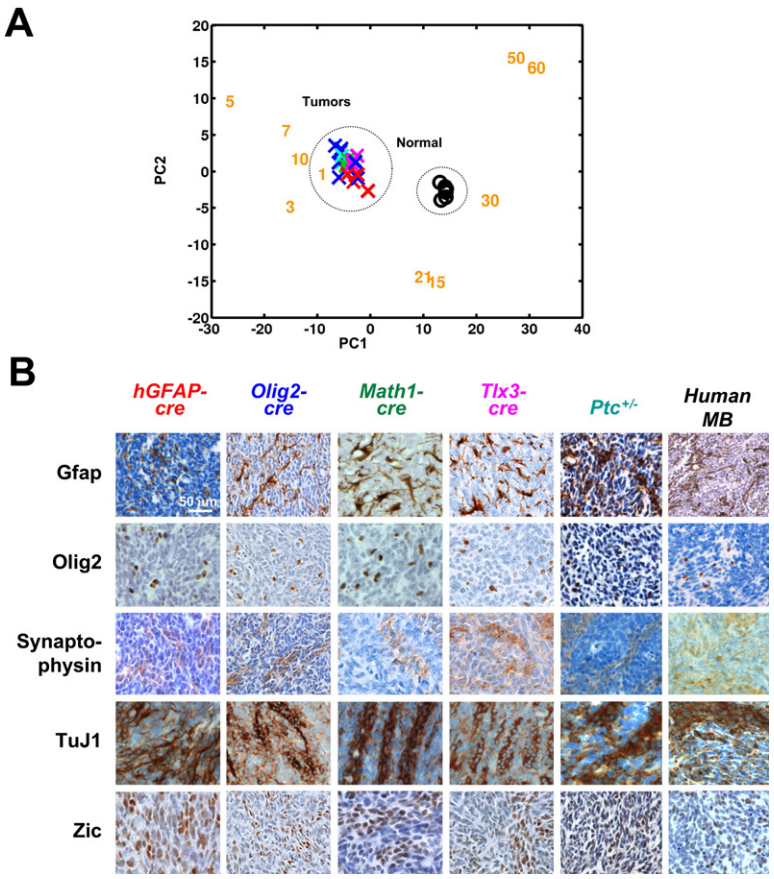

Figure 5. Medulloblastoma Generated from Diverse Progenitor Cell Origins Leads to a Convergent Phenotypic Endpoint

(A) Principal component analysis of global gene expression in conditional MB models (*hGFAP*- [red], *Olig2*- [blue], *Math1*- [green], *Tlx3-cre:SmoM2* [magenta], and $Ptc^{+/-}$ [turquoise]) and samples from normal littermate control CB (black circles) mapped onto normal cerebellar developmental space as defined by a 7000 member, rank-normalized gene set (Kho et al., 2004) from developing CB at stages P1, 3, 5, 7, 10, 15, 21, 30, 50, and 60 (orange numbers). Tumors were related to early rather than late developmental stages of the CB as we have reported previously for human MB (Kho et al., 2004).

(B) Immunohistochemical analysis confirms that all murine tumors exhibit an immunohistochemical staining pattern similar to each other as well as human MB with respect to standard neuronal and glial neuropathological markers. Results are representative of at least two tumor samples.

MB. These findings provide insight into MB origins with implications for development of targeted cellular therapies.

Olig2$^+$ Progenitors of the RL Give Rise to a Subset of Granule Cell Neurons

By creating a knockin transgenic mouse line, *Olig2-tva-cre*, we targeted Olig2$^+$ cells using two fate-mapping approaches. *Olig2-tva-cre* intercrossed with conditional reporters (e.g., *ROSA26-YFP*) mapped a subset of GCs in the EGL and IGL of posterior CB. We then confirmed that these cells were derived from Olig2$^+$ progenitors in the rRL by in utero infection of *Olig2-tva-cre* mice with an avian RCAS retrovirus reporter. Although we cannot exclude that Olig2$^+$ cells outside of the rRL could contribute to CGNPs, this possibility seems unlikely given previous work that has established the rRL as the source of the GC lineage. These data indicate that rRL Olig2$^+$ progenitors give rise to a subset of GCs (Figure S5A) that might contribute to functional heterogeneity (Zong et al., 2005).

Oncogenic Signaling and Lineage-Restricted Factors Cooperate to Determine Tumor Competence in CNS Progenitors

Human inherited cancer syndromes exhibit tumor formation in only a subset of cells within specific lineages despite germline transmission of tumor-promoting mutations (e.g., *p53*, *pRB* loss of function). Although several reports indicate that the Hh pathway is active in low- and high-grade gliomas (Ehtesham et al., 2007; Clement et al., 2007), in human Goltz-Gorlin syndrome, inherited heterozygous mutation of *PTC* or *SUFU* leads to MB but not glioma. We failed to detect gliomas despite robust SmoM2 activation in forebrain progenitors, including developing neural stem cells and persistent progenitors of the SVZ and cortex expressing GFAP (Doetsch et al., 1999), NG2/Olig2 (Ligon et al., 2006), and Gli1 (Machold et al., 2003; Ahn and Joyner, 2005). Further work is needed to establish whether additional mutations (e.g., loss of *p53*) in concert with Hh activation might be necessary to enable glioma formation. Another possibility is that Shh activation biases toward neuronal lineage versus glial differentiation and therefore a MB phenotype and not glial lineages or glial tumor phenotype. Although we cannot rule this out, we think that this explanation is unlikely for the following reasons. First, if one assumes that Shh promotes neuronal tumorigenesis, then one might expect to see development of such tumors at other CNS sites (e.g., supratentorial PNETs); this is not observed in human Goltz-Gorlin syndrome patients or in the mouse models that we have studied. Second, we did not see other neuronal tumor types in the CB despite activation of Shh in PNs and INs (Table 1). Third, we have recently shown that SmoM2 activation in the dentate gyrus causes hypertrophy but not cancer (Han et al., 2008).

Acquisition of Granule Cell Lineage Identity Is Critical for Hh-Induced Medulloblastoma Formation

To identify progenitors competent for MB formation, we activated SmoM2 in a spectrum of stage- and position-specific progenitors during CGNP development. Both multipotent (e.g., *hGFAP*$^+$ and *Olig2*$^+$) progenitor populations within the cerebellar anlage as well as unipotent/restricted CGNPs readily gave rise to MB with 100% penetrance. Despite these diverse origins, all SmoM2-activated MBs that we analyzed exhibited a strikingly similar tumor phenotype at histological, immunohistochemical, and expression profiling levels. The common final tumor phenotype is consistent with (1) a common cell of origin for all tumors or (2) initial origins from any stem/progenitor that later converge on

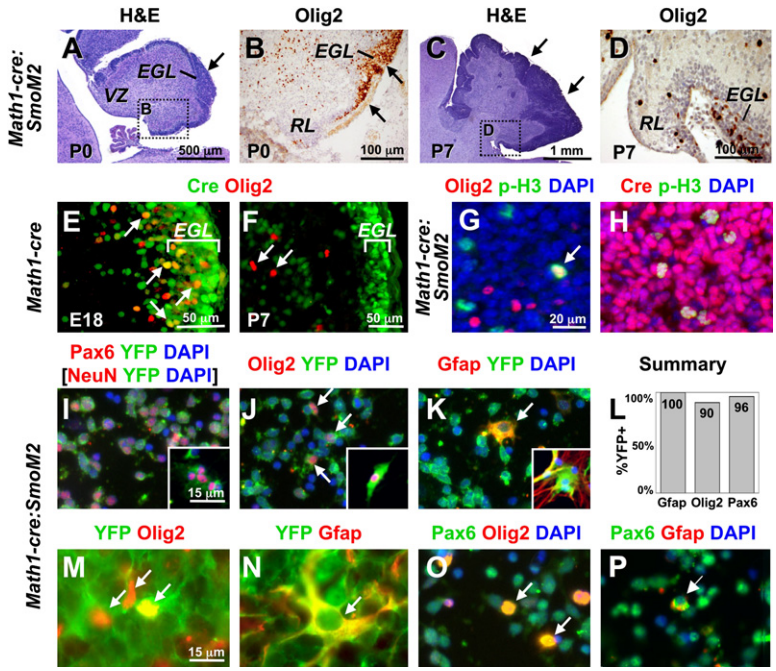

Figure 6. Olig2- and Gfap-Expressing Cells in Medulloblastoma Are Neoplastic and Have Features in Common with Immature Granule Lineage Precursors

(A and C) In *Math1-cre:SmoM2* animals, morphologic evidence of hyperplasia is predominantly observed in the EGL—but not in the RL or VZ—at P0 and is more apparent by P7.

(B and D) Greatly increased numbers of Olig2$^+$ cells are observed in hyperplastic regions of the EGL—but not in the RL—of P0 and P7 *Math1-cre:SmoM2* mice.

(E and F) Expression of Cre proteins in *Math1-cre* mice colocalized with Olig2 at E18, but not at P7.

(G) Olig2 coexpression was detected in only ~2% of phospho-H3 (p-H3)$^+$ cells in tumors.

(H) In contrast, ~98% of p-H3$^+$ cells colabeled with Cre proteins.

(I–K) Phenotype of acutely disassociated cells and cells cultured from MB for 4 weeks (insets). While most dissociated *Math1-cre:SmoM2* tumor cells express the GC markers Pax6 (I) or NeuN (inset in I), some express Olig2 (J) and Gfap (K). SmoM2 is fused to YFP, which therefore marks tumor cells.

(L) Cell counting reveals that more than 90% of cells expressing Gfap, Olig2, and Pax6 are tumor cells, as shown by coexpression of YFP.

(M and N) Immunohistochemistry of tumor sections demonstrates similar results.

(O and P) 81% of Olig2$^+$ (O) and 100% of Gfap$^+$ (P) cells in tumors express the CGNP marker Pax6.

an amplifying CGNP-like tumor cell that dominates the ultimate phenotype (see Figure S5C). In either case, these findings support the conclusion that acquisition of CGNP identity is important for Hh-induced MB formation. Because orthotopically transplanted *Olig2-tva-cre:SmoM2* tumors were able to grow within the forebrain and CB, restriction of tumor susceptibility is evidently governed by cell-intrinsic factors. Further work is needed to identify the underlying molecular determinants of CGNP tumor competence that lead to MB formation.

Hh-Activated Medulloblastoma Can Be Generated in the EGL Independent of VZ Contributions

Human desmoplastic MB and classic MB have been suggested to arise from EGL CGNPs (Schüller et al., 2005; Bühren et al., 2000) and progenitors of the VZ (Salsano et al., 2007; Katsetos et al., 1995), respectively. Our studies demonstrate that Hh-induced MB can be initiated by precise restriction of activating mutations to the EGL using *Tlx3-cre:SmoM2* and postnatally induced *Gli1-creERT2:SmoM2* without activation of SmoM2 in the less differentiated cell populations of the rRL or VZ. Furthermore, while the time of tumor onset and the degree of tumor distribution varied depending on the Cre drivers used (Table 1; Figure S5B), these variations appear to be based on the number, extent, and/or location of the total CGNP population targeted (i.e., broad diffuse versus small lateral populations). In addition, tumor masses did not develop in the VZ or rRL proper, suggesting that further work will be needed to determine whether additional oncogenic pathways (e.g., MYC or Wnt) might lead to MB formation in these regions.

Evidence that Gfap$^+$ and Olig2$^+$ Cells in Medulloblastomas Are Neoplastic

Our data highlight that both mouse and human MBs exhibit extensive cellular heterogeneity. GFAP$^+$ cells are commonly identified in human MB (Schüller et al., 2004), and the morphology of these cells ranges from small tumor cells with a relatively large nucleus and a sparse, ring-like cytoplasm to cells with a rather differentiated phenotype and branched processes. We observed that OLIG2$^+$ cells, present in human MB, also varied in size and morphology. Using MYC FISH in human MB and YFP tracer expression in murine MB, we have demonstrated that OLIG2$^+$ and GFAP$^+$ cells are bona fide tumor cells and not just infiltrating cells arising from the normal surrounding brain. In addition, we found small numbers of proliferating Olig2$^+$ and Gfap$^+$ cells within mouse MB and, to a lesser degree, human MB, further evidence that these heterogeneous elements represent tumor cells.

In human gliomas, OLIG2 is expressed in tumor stem/progenitor cells, and Olig2 maintains the proliferation competence of both normal and tumorigenic progenitors of the murine forebrain (Ligon et al., 2007). However, given our data indicating that OLIG2 is only rarely expressed in proliferating cells and is only present in 40% of classic and 77% of desmoplastic human MB cases, it seems clear that MB tumor growth is driven largely by rapidly dividing progenitor cells with CGNP characteristics rather than by OLIG2$^+$ cells. Might GFAP$^+$ and OLIG2$^+$ cells in MB have other roles as relatively quiescent tumor progenitor cells? Our in vitro tumor fate mapping demonstrates that Hh-transformed Olig2$^+$ cells from murine MB can produce GC lineage-like progeny with advanced differentiation as measured by NeuN labeling. Whether Olig2$^+$ tumor cells from other mouse models (i.e., non-*Olig2-cre*-derived) have this capability remains to be determined.

Our data suggest that GFAP and OLIG2 expression in MB are not associated with "differentiated" ASs and OLs. While almost all Gfap$^+$ and Olig2$^+$ cells in Hh-activated murine MB coexpressed Pax6 and other CGNP markers, the "biphenotypic" (e.g., OLIG2-NEUN) staining pattern is unlikely to be a specific consequence of Hh signaling because we also observed this

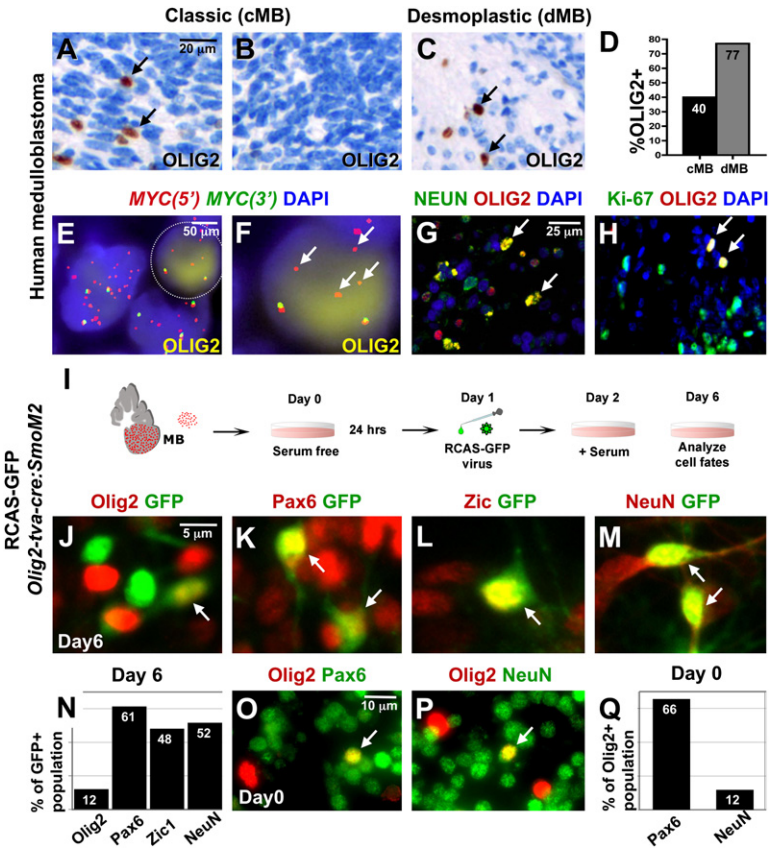

Figure 7. OLIG2 Is Expressed in Human Medulloblastoma

(A–D) OLIG2 expression in human classic and desmoplastic MB (A–C) and percentage of tumors of each class that contain OLIG2$^+$ cells (D) (see also Table S1).

(E and F) Combined FISH and immunohistochemical analysis reveals the presence of tumor-specific c-*MYC* genomic aberrations (Herms et al., 2000) within OLIG2$^+$ cells (yellow nuclei) of human MB (n = 2). c-*MYC* aberrations were identical in OLIG2$^+$ and OLIG2$^-$ tumor cells. Note combined copy-number gain (red signals, 5′ c-*MYC*) and structural aberration (loss of green signals, 3′ c-*MYC*) as detected using a break-apart probe set. Normal MYC loci show merged colors as yellow focal signals.

(G and H) OLIG2 colocalizes with NEUN and the proliferation marker Ki-67.

(I) Scheme for experiments using RCAS-GFP infection of *Olig2-tva-cre:SmoM2* tumor cells.

(J–M) Double-fluorescence images show expression of GFP that colocalizes with immunoreactivity using antibodies against Olig2 and GC markers. Note that while *Olig2-tva-cre:SmoM2* cells express YFP, the signal is very weak/undetectable compared with GFP encoded by the RCAS virus.

(N) Summary of findings at day 6 in GFP-labeled cells.

(O–Q) Analysis of acutely disassociated *Olig2-tva-cre:SmoM2* tumor cells (day 0). Of Olig2$^+$ cells, 66% colabeled with Pax6 and 12% with NeuN; such cells represented 4% and 1% of total cells in the tumor, respectively.

phenomenon in classic MBs, which are not associated with Hh mutations (Pietsch et al., 1997). We suggest that GFAP and OLIG2 label cells with a phenotype reminiscent of radial glia and less differentiated CGNP progenitors of the rRL (Figure S5A).

Does Medulloblastoma Arise from a Multipotent Stem Cell?

MB was one of the first solid tumors for which "cancer stem cells" were reported (Hemmati et al., 2003). Cancer stem cells are classically described as a tumor subpopulation with (1) unlimited capacity for self-renewal and the ability to regenerate tumors upon transplantation and (2) the potential to produce multilineage progeny similar to distinct cell types of a cognate organ (Reya et al., 2001). The question of authentic glial cell production has critical implications for understanding MB progenitors and their characterization as multipotent cancer stem cells. However, evidence for multilineage differentiation of MB stem cells has been based on the expression of relatively few neuronal and glial cell markers with uncertain relation to either differentiated cell types of the CB or CNS multipotent stem cells. For example, the commonly used marker GFAP marks type B stem cells of the SVZ (Doetsch et al., 1999). We show that Gfap and Olig2 mark cells in MBs reminiscent of those found during early CGNP development, but not differentiated glia. These findings argue against existence of MB progenitors with multilineage (neuronal and glial) contributions to tumor mass. However, they are consistent with the possibility that MB could originate from either a multipotent or a unipotent progenitor (Figure S5C).

We used lineage tracing to clarify the possible relationship between cells found during GC lineage development and those that are tumor competent to produce MB. Our findings highlight distinctions between the "cell of origin" (which acquires the oncogenic mutation) and "tumor-propagating" cells, responsible for major growth and phenotypic characteristics of the ultimate tumor. For instance, if unipotent cell identity ("type C2") is necessary for tumor growth (Figure S5C), then a tumor arising from mutation of a type A cell or a type C2 cell should appear identical, notwithstanding their different cells of origin. This also raises the possibility of a "dedifferentiation" pathway that produces tumors with mixed multipotent and unipotent features, as has been suggested for certain leukemia stem cells (Krivtsov et al., 2006). Although our data do not provide direct evidence for dedifferentiation, tumors from postnatally induced *Gli1-creERT2:SmoM2* (J.M., A.P.M., and K.L., unpublished data) and *Math1-creERT2:Ptc$^{flox/flox}$* animals (Z.-J. Yang and R.J. Wechsler-Reya, personal communication) contain many Olig2$^+$ cells, consistent with the possibility that late-stage CGNPs can adopt less differentiated characteristics (Figure S5). Further investigation is needed to determine whether dedifferentiation of mature granule cells (D2 → C2; see Figure S5C) constitutes a biologically feasible or clinically relevant pathway of tumor formation.

EXPERIMENTAL PROCEDURES

Animal Procedures

For fate mapping, various *cre* strains (Table 1) were intercrossed with *ROSA26-eYFP$^{flox/flox}$* or *CAG-CAT-eGFP$^{flox/flox}$* conditional reporter mice. At

least three cerebella were harvested for each different time point and fixed overnight in 4% paraformaldehyde/PBS. For tumor generation, *cre* strains were intercrossed with *SmoM2*$^{flox/flox}$ mice and followed for survival and subsequent Kaplan-Meier analysis. For injections into forebrains or cerebella of SCID mice, tumor cells were freshly dissociated and resuspended in 1 μl PBS at a concentration of 10^5/μl (see Supplemental Experimental Procedures). See Supplemental Experimental Procedures for detailed information on generation, acquisition, and genotyping of transgenic mouse strains and procedures including RCAS infection of *Olig2-tva-cre* embryonic hindbrain. All animal procedures were approved by the Institutional Animal Care and Use Committees of the Dana-Farber Cancer Institute and the University of California, San Francisco.

Tissue Collection, Histological Analysis, Immunohistochemistry, In Situ Hybridization, and Photomicroscopy

Human tissue samples were obtained in accordance with the rules and regulations for human tissue collection and use at Children's Hospital Boston, Brigham and Women's Hospital/Partners HealthCare, and University Hospital München-Großhadern. Tissue samples were processed using standard techniques. Detailed protocols for in situ hybridization, immunohistochemistry, and immuno-FISH as well as all antibodies used in this study are listed in Supplemental Experimental Procedures. Photomicrographs were acquired with Zeiss Axioskop/Axiocam or Nikon E600/SPOT imaging systems. For whole-mount images of mouse MBs, fluorescence and bright-field images were overlaid using Adobe Photoshop software. A Leica TCS SL system was used for confocal microscopy.

Cell Culture

Cultures from *Math1-cre:SmoM2* tumors were established by triturating tumor tissue in DMEM and plating the cells on poly-D-lysine-coated dishes. Acutely dissociated *Math1-cre:SmoM2* tumor cells were fixed 12 hr after plating. Long-term cultures were analyzed after 4 weeks in culture and three passages. Immunostaining was performed as described above. Cells from *Olig2-tva-cre:SmoM2* tumors were infected with virus carrying *RCAS(A)-GFP* (2×10^7 cfu/ml; gift of C. Cepko, Harvard Medical School) after 24 hr culture in serum-free medium. Serum-containing medium was then added, and after a total culture time of 6 days, cells were fixed and stained.

Statistics and Quantification

For in vivo fate mapping in *Olig2-tva-cre* mice, counts were derived from analyses of three independent animals and at least ten 20× fields of labeled sections of CB focused around lobe X. For cell culture counts, cells were derived from pups from at least four separate litters. Each litter yielded material for two six-well plates of cerebellar cultures and one six-well plate of ventricular cultures. EGF, Shh, and vehicle were each applied to three 3.5 cm culture wells. At least 100 cells were assessed in each sample to determine the fraction of Olig2$^+$, Zic$^+$, and Gfap$^+$ cells. Statistical analysis was performed using Student's unpaired t test with a two-tailed p value.

Microarray Data and Analysis

The transcriptomes of 21 Cre-activated tumors and control cerebellar tissues were profiled using the Affymetrix GeneChip Mouse Genome 430 2.0 Plus array. Transcriptomes of the P1–60 developing mouse CB were profiled using the Affymetrix Murine Mu11K set as described previously (Kho et al., 2004), and principal component analysis was used to determine the global similarity and variation between the transcriptome profiles of the different tissues (Johnson and Wichern, 2002). For detailed description, see Supplemental Experimental Procedures.

ACCESSION NUMBERS

Microarray data have been deposited in the NCBI Gene Expression Omnibus (http://www.ncbi.nlm.nih.gov/geo/) with the accession number GSE11859.

SUPPLEMENTAL DATA

The Supplemental Data include Supplemental Experimental Procedures, Supplemental References, one table, and five figures and can be found with this article online at http://www.cancercell.org/cgi/content/full/14/2/123/DC1/.

ACKNOWLEDGMENTS

The authors are grateful to R.J. Wechsler-Reya for sharing unpublished data; C.D. Stiles for comments; and J. Ling, S. Kaing, D.-i. Yuk, N. Vena, and E. Learner for expert technical assistance. U.S. was supported by a fellowship from the Dr. Mildred-Scheel-Stiftung für Krebsforschung and by the Max-Eder-Nachwuchsgruppenprogramm of the Deutsche Krebshilfe. V.M.H. thanks the Netherlands Organization for Scientific Research (NWO) for a TALENT stipend. J.M. was supported by a grant from the Charles King Trust/Medical Foundation. A.K.D., Y-G.H., and E.H. thank the American Brain Tumor Association for support. This work was supported by grants from the NIH to K.L.L. (NS047213), A.T.K. (NS040828), A.P.M. (NS033642), and D.H.R. (NS047527); the James S. McDonnell Foundation (to D.H.R.); the March of Dimes Foundation (to D.H.R.); and the Pediatric Brain Tumor Foundation of the United States (to A.A.-B. and D.H.R.). D.H.R. is a Howard Hughes Medical Institute Investigator.

Received: January 27, 2008
Revised: June 3, 2008
Accepted: July 10, 2008
Published: August 11, 2008

REFERENCES

Abraham, H., Tornoczky, T., Kosztolanyi, G., and Seress, L. (2001). Cell formation in the cortical layers of the developing human cerebellum. Int. J. Dev. Neurosci. *19*, 53–62.

Ahn, S., and Joyner, A.L. (2005). In vivo analysis of quiescent adult neural stem cells responding to Sonic hedgehog. Nature *437*, 894–897.

Altmann, J., and Bayer, S.A. (1997). Development of the Cerebellar System: In Relation to Its Evolution, Structure, and Functions (New York: CRC Press).

Barabe, F., Kennedy, J.A., Hope, K.J., and Dick, J.E. (2007). Modeling the initiation and progression of human acute leukemia in mice. Science *316*, 600–604.

Ben Arie, N., Bellen, H.J., Armstrong, D.L., McCall, A.E., Gordadze, P.R., Guo, Q., Matzuk, M.M., and Zoghbi, H.Y. (1997). Math1 is essential for genesis of cerebellar granule neurons. Nature *390*, 169–172.

Borghesani, P.R., Peyrin, J.M., Klein, R., Rubin, J., Carter, A.R., Schwartz, P.M., Luster, A., Corfas, G., and Segal, R.A. (2002). BDNF stimulates migration of cerebellar granule cells. Development *129*, 1435–1442.

Bühren, J., Christoph, A.H., Buslei, R., Albrecht, S., Wiestler, O.D., and Pietsch, T. (2000). Expression of the neurotrophin receptor p75NTR in medulloblastomas is correlated with distinct histological and clinical features: evidence for a medulloblastoma subtype derived from the external granule cell layer. J. Neuropathol. Exp. Neurol. *59*, 229–240.

Casper, K.B., and McCarthy, K.D. (2006). GFAP-positive progenitor cells produce neurons and oligodendrocytes throughout the CNS. Mol. Cell. Neurosci. *31*, 676–684.

Clement, V., Sanchez, P., de Tribolet, N., Radovanovic, I., and Altaba, A. (2007). HEDGEHOG-GLI1 signaling regulates human glioma growth, cancer stem cell self-renewal, and tumorigenicity. Curr. Biol. *17*, 165–172.

Cobaleda, C., Jochum, W., and Busslinger, M. (2007). Conversion of mature B cells into T cells by dedifferentiation to uncommitted progenitors. Nature *449*, 473–477.

Dahmane, N., and Altaba, A. (1999). Sonic hedgehog regulates the growth and patterning of the cerebellum. Development *126*, 3089–3100.

Doetsch, F., Caille, I., Lim, D.A., Garcia-Verdugo, J.M., and Alvarez-Buylla, A. (1999). Subventricular zone astrocytes are neural stem cells in the adult mammalian brain. Cell *97*, 703–716.

Ehtesham, M., Sarangi, A., Valadez, J.G., Chanthaphaychith, S., Becher, M.W., Abel, T.W., Thompson, R.C., and Cooper, M.K. (2007). Ligand-dependent activation of the hedgehog pathway in glioma progenitor cells. Oncogene *26*, 5752–5761.

Engelkamp, D., Rashbass, P., Seawright, A., and van Heyningen, V. (1999). Role of Pax6 in development of the cerebellar system. Development *126*, 3585–3596.

Faber, J., and Armstrong, S.A. (2007). Mixed lineage leukemia translocations and a leukemia stem cell program. Cancer Res. *67*, 8425–8428.

Fuccillo, M., Joyner, A.L., and Fishell, G. (2006). Morphogen to mitogen: the multiple roles of hedgehog signalling in vertebrate neural development. Nat. Rev. Neurosci. *7*, 772–783.

Galli, R., Binda, E., Orfanelli, U., Cipelletti, B., Gritti, A., De Vitis, S., Fiocco, R., Foroni, C., DiMeco, F., and Vescovi, A. (2004). Isolation and characterization of tumorigenic, stem-like neural precursors from human glioblastoma. Cancer Res. *64*, 7011–7021.

Hahn, H., Wojnowski, L., Miller, G., and Zimmer, A. (1999). The patched signaling pathway in tumorigenesis and development: lessons from animal models. J. Mol. Med. *77*, 459–468.

Han, Y.G., Spassky, N., Romaguera-Ros, M., Garcia-Verdugo, J.M., Aguilar, A., Schneider-Maunoury, S., and Alvarez-Buylla, A. (2008). Hedgehog signaling and primary cilia are required for the formation of adult neural stem cells. Nat. Neurosci. *11*, 277–284.

Hemmati, H.D., Nakano, I., Lazareff, J.A., Masterman-Smith, M., Geschwind, D.H., Bronner-Fraser, M., and Kornblum, H.I. (2003). Cancerous stem cells can arise from pediatric brain tumors. Proc. Natl. Acad. Sci. USA *100*, 15178–15183.

Herms, J., Neidt, I., Lüscher, B., Sommer, A., Schurmann, P., Schröder, T., Bergmann, M., Wilken, B., Probst-Cousin, S., Hernaiz-Driever, P., et al. (2000). C-MYC expression in medulloblastoma and its prognostic value. Int. J. Cancer *89*, 395–402.

Johnson, R.A., and Wichern, D.W. (2002). Applied Multivariate Statistical Analysis (Upper Saddle River, NJ, USA: Prentice Hall).

Johnson, R.L., Rothman, A.L., Xie, J., Goodrich, L.V., Bare, J.W., Bonifas, J.M., Quinn, A.G., Myers, R.M., Cox, D.R., Epstein, E.H., Jr., and Scott, M.P. (1996). Human homolog of patched, a candidate gene for the basal cell nevus syndrome. Science *272*, 1668–1671.

Katsetos, C.D., Herman, M.M., Krishna, L., Vender, J.R., Vinores, S.A., Agamanolis, D.P., Schiffer, D., Burger, P.C., and Urich, H. (1995). Calbindin-D28k in subsets of medulloblastomas and in the human medulloblastoma cell line D283 Med. Arch. Pathol. Lab. Med. *119*, 734–743.

Kawauchi, D., Taniguchi, H., Watanabe, H., Saito, T., and Murakami, F. (2006). Direct visualization of nucleogenesis by precerebellar neurons: involvement of ventricle-directed, radial fibre-associated migration. Development *133*, 1113–1123.

Kho, A.T., Zhao, Q., Cai, Z., Butte, A.J., Kim, J.Y., Pomeroy, S.L., Rowitch, D.H., and Kohane, I.S. (2004). Conserved mechanisms across development and tumorigenesis revealed by a mouse development perspective of human cancers. Genes Dev. *18*, 629–640.

Krivtsov, A.V., Twomey, D., Feng, Z., Stubbs, M.C., Wang, Y., Faber, J., Levine, J.E., Wang, J., Hahn, W.C., Gilliland, D.G., et al. (2006). Transformation from committed progenitor to leukaemia stem cell initiated by MLL-AF9. Nature *442*, 818–822.

Lee, A., Kessler, J.D., Read, T.A., Kaiser, C., Corbeil, D., Huttner, W.B., Johnson, J.E., and Wechsler-Reya, R.J. (2005). Isolation of neural stem cells from the postnatal cerebellum. Nat. Neurosci. *8*, 723–729.

Lee, Y., Miller, H.L., Jensen, P., Hernan, R., Connelly, M., Wetmore, C., Zindy, F., Roussel, M.F., Curran, T., Gilbertson, R.J., and McKinnon, P.J. (2003). A molecular fingerprint for medulloblastoma. Cancer Res. *63*, 5428–5437.

Lewis, P.M., Gritli-Linde, A., Smeyne, R., Kottmann, A., and McMahon, A.P. (2004). Sonic hedgehog signaling is required for expansion of granule neuron precursors and patterning of the mouse cerebellum. Dev. Biol. *270*, 393–410.

Ligon, K.L., Kesari, S., Kitada, M., Sun, T., Arnett, H.A., Alberta, J.A., Anderson, D.J., Stiles, C.D., and Rowitch, D.H. (2006). Development of NG2 neural progenitor cells requires Olig gene function. Proc. Natl. Acad. Sci. USA *103*, 7853–7858.

Ligon, K.L., Huillard, E., Mehta, S., Kesari, S., Liu, H., Alberta, J.A., Bachoo, R.M., Kane, M., Louis, D.N., Depinho, R.A., et al. (2007). Olig2-regulated lineage-restricted pathway controls replication competence in neural stem cells and malignant glioma. Neuron *53*, 503–517.

Lu, Q.R., Sun, T., Zhu, Z., Ma, N., Garcia, M., Stiles, C.D., and Rowitch, D.H. (2002). Common developmental requirement for Olig function indicates a motor neuron/oligodendrocyte connection. Cell *109*, 75–86.

Machold, R., and Fishell, G. (2005). Math1 is expressed in temporally discrete pools of cerebellar rhombic-lip neural progenitors. Neuron *48*, 17–24.

Machold, R., Hayashi, S., Rutlin, M., Muzumdar, M.D., Nery, S., Corbin, J.G., Gritli-Linde, A., Dellovade, T., Porter, J.A., Rubin, L.L., et al. (2003). Sonic hedgehog is required for progenitor cell maintenance in telencephalic stem cell niches. Neuron *39*, 937–950.

Malatesta, P., Hack, M.A., Hartfuss, E., Kettenmann, H., Klinkert, W., Kirchhoff, F., and Götz, M. (2003). Neuronal or glial progeny: regional differences in radial glia fate. Neuron *37*, 751–764.

Mao, J., Ligon, K.L., Rakhlin, E.Y., Thayer, S.P., Bronson, R.T., Rowitch, D., and McMahon, A.P. (2006). A novel somatic mouse model to survey tumorigenic potential applied to the Hedgehog pathway. Cancer Res. *66*, 10171–10178.

Matei, V., Pauley, S., Kaing, S., Rowitch, D., Beisel, K.W., Morris, K., Feng, F., Jones, K., Lee, J., and Fritzsch, B. (2005). Smaller inner ear sensory epithelia in Neurog 1 null mice are related to earlier hair cell cycle exit. Dev. Dyn. *234*, 633–650.

Morales, D., and Hatten, M.E. (2006). Molecular markers of neuronal progenitors in the embryonic cerebellar anlage. J. Neurosci. *26*, 12226–12236.

Petryniak, M.A., Potter, G.B., Rowitch, D.H., and Rubenstein, J.L. (2007). Dlx1 and Dlx2 control neuronal versus oligodendroglial cell fate acquisition in the developing forebrain. Neuron *55*, 417–433.

Pietsch, T., Waha, A., Koch, A., Kraus, J., Albrecht, S., Tonn, J., Sörensen, N., Berthold, F., Henk, B., Schmandt, N., et al. (1997). Medulloblastomas of the desmoplastic variant carry mutations of the human homologue of Drosophila patched. Cancer Res. *57*, 2085–2088.

Pomeroy, S.L., Tamayo, P., Gaasenbeek, M., Sturla, L.M., Angelo, M., McLaughlin, M.E., Kim, J.Y., Goumnerova, L.C., Black, P.M., Lau, C., et al. (2002). Prediction of central nervous system embryonal tumour outcome based on gene expression. Nature *415*, 436–442.

Reya, T., Morrison, S.J., Clarke, M.F., and Weissman, I.L. (2001). Stem cells, cancer, and cancer stem cells. Nature *414*, 105–111.

Rowitch, D.H., Jacques, B., Lee, S.M., Flax, J.D., Snyder, E.Y., and McMahon, A.P. (1999). Sonic hedgehog regulates proliferation and inhibits differentiation of CNS precursor cells. J. Neurosci. *19*, 8954–8965.

Salsano, E., Croci, L., Maderna, E., Lupo, L., Pollo, B., Giordana, M.T., Consalez, G.G., and Finocchiaro, G. (2007). Expression of the neurogenic basic helix-loop-helix transcription factor NEUROG1 identifies a subgroup of medulloblastomas not expressing ATOH1. Neuro-oncol. *9*, 298–307.

Schüller, U., Schober, F., Kretzschmar, H.A., and Herms, J. (2004). Bcl-2 expression inversely correlates with tumour cell differentiation in medulloblastoma. Neuropathol. Appl. Neurobiol. *30*, 513–521.

Schüller, U., Koch, A., Hartmann, W., Garre, M.L., Goodyer, C.G., Cama, A., Sörensen, N., Wiestler, O.D., and Pietsch, T. (2005). Subtype-specific expression and genetic alterations of the chemokinereceptor gene CXCR4 in medulloblastomas. Int. J. Cancer *117*, 82–89.

Shih, A.H., and Holland, E.C. (2004). Developmental neurobiology and the origin of brain tumors. J. Neurooncol. *70*, 125–136.

Singh, S.K., Hawkins, C., Clarke, I.D., Squire, J.A., Bayani, J., Hide, T., Henkelman, R.M., Cusimano, M.D., and Dirks, P.B. (2004). Identification of human brain tumour initiating cells. Nature *432*, 396–401.

Spassky, N., Han, Y.G., Aguilar, A., Strehl, L., Besse, L., Laclef, C., Romaguera, R.M., Garcia-Verdugo, J.M., and Alvarez-Buylla, A. (2008). Primary cilia are required for cerebellar development and Shh-dependent expansion of progenitor pool. Dev. Biol. *317*, 246–259.

Srinivas, S., Watanabe, T., Lin, C.S., William, C.M., Tanabe, Y., Jessell, T.M., and Costantini, F. (2001). Cre reporter strains produced by targeted insertion of EYFP and ECFP into the ROSA26 locus. BMC Dev. Biol. *1*, 4.

Wang, V.Y., Rose, M.F., and Zoghbi, H.Y. (2005). Math1 expression redefines the rhombic lip derivatives and reveals novel lineages within the brainstem and cerebellum. Neuron *48*, 31–43.

Warner, J.K., Wang, J.C., Hope, K.J., Jin, L., and Dick, J.E. (2004). Concepts of human leukemic development. Oncogene *23*, 7164–7177.

Wechsler-Reya, R.J., and Scott, M.P. (1999). Control of neuronal precursor proliferation in the cerebellum by Sonic Hedgehog. Neuron *22*, 103–114.

Xu, Y., Lopes, C., Qian, Y., Cheng, L., Goulding, M., Turner, E., Lima, D., and Ma, Q. (2008). Tlx1 and Tlx3 coordinate specification of dorsal horn pain-modulary peptidergic neurons. J. Neurosci. *28*, 4037–4046.

Yamasaki, T., Kawaji, K., Ono, K., Bito, H., Hirano, T., Osumi, N., and Kengaku, M. (2001). Pax6 regulates granule cell polarization during parallel fiber formation in the developing cerebellum. Development *128*, 3133–3144.

Yang, Z.-J., Ellis, T., Markant, S.L., Read, T.-A., Kessler, J.D., Bourboulas, M., Schüller, U., Machold, R., Fishell, G., Rowitch, D.H., et al. (2008). Medulloblastoma can be initiated by deletion of *patched* in lineage-restricted progenitors or stem cells. Cancer Cell *14*, this issue, 135–145.

Zhou, Q., and Anderson, D.J. (2002). The bHLH transcription factors OLIG2 and OLIG1 couple neuronal and glial subtype specification. Cell *109*, 61–73.

Zong, H., Espinosa, J.S., Su, H.H., Muzumdar, M.D., and Luo, L. (2005). Mosaic analysis with double markers in mice. Cell *121*, 479–492.